JOURNAL OF GEOPHYSICAL RESEARCH, VOL. 98, NO. A12, PAGES 21,189-21,202, DECEMBER 1, 1993

Ulysses Plasma Observations in the Jovian Magnetosheath

J. L. PHILLIPS, S. J. BAME, AND M. F. THOMSEN

Los Alamos National Laboratory, Los Alamos, New Mexico

B. E. GOLDSTEIN AND E. J. SMITH

Jet Propulsion Laboratory, Pasadena, California

The solar wind plasma experiment aboard the Ulysses spacecraft, including separate ion and electron instruments, measured the plasma properties of the Jovian magnetosheath during the February 1992 encounter with Jupiter. Seven separate magnetosheath intervals were observed, as well as four bow shock crossings and numerous encounters with the magnetopause and its boundary layer. We present an overview of ion and electron bulk parameters and a sampling of distribution shapes for the magnetosheath and adjacent plasma regions. Plasma flows are generally appropriate for slowing and deflection of the solar wind flow about a relatively stationary obstacle, with the notable exception of the first inbound sheath transit, when an expanding magnetosphere resulted in sunward flow just above the magnetopause. The existence of a planetary depletion layer is suggested by trends in plasma density for some magnetopause encounters. The magnetopause boundary layer is characterized by a combination of sheathlike and magnetospheric distributions of both ions and electrons. The ion population in the sheath is observed to include a significant population of suprathermal protons. Electron distributions have a distinctive shape previously observed in the terrestrial magnetosheath, with fluxes parallel to the magnetic field dominating at thermal energies and perpendicular fluxes dominating at higher energies. Trends in electron temperature near the bow shock indicate that shock motion plays an important role in heating the electrons. In general, the plasma characteristics of the Jovian magnetosheath are quite similar to those in its terrestrial counterpart, but the compressible nature of the Jovian magnetosphere accentuates the importance of boundary motions.

INTRODUCTION

Each of the planets thus far encountered by spacecraft, from Mercury through Neptune, has been observed to have a planetary bow shock which heats, compresses, and deflects the oncoming solar plasma. The region of shocked solar plasma downstream of a planetary bow shock is known as the magnetosheath, although the term ionosheath is sometimes used for nonmagnetized planets (most notably Venus and possibly also Mars) for which the obstacle to the solar wind flow is ionospheric rather than magnetospheric. For a magnetized planet such as Jupiter the dayside and near-terminator magnetosheath can be defined as the region between the bow shock and the magnetopause; the existence of transition regions and boundary layers complicates this simple definition somewhat.

The magnetosheath of Jupiter has been sampled by plasma instrumentation on board Pioneer 10 and 11 [e.g., *Intriligator and Wolfe*, 1976] and Voyager 1 and 2 [e.g. *Scudder et al.*, 1981; *Richardson*, 1987]. Some of the results include (1) a proton temperature of 2-10 x 10^5 K and the presence of a substantial electron population in the energy range of 50-200 eV [*Intriligator and Wolfe*, 1976]; (2) presence of a suprathermal proton component, raising the total proton temperature above 10^6 K [*Richardson*, 1987]; (3) electron temperatures of 2-7 x 10^5 K, with flat-topped distribution shapes similar to those seen in Earth's magnetosheath [*Scudder et al.*, 1981]; (4) the presence of a magnetopause boundary layer in which the plasma characteristics transition gradually from magnetosheathlike to magnetospherelike [*Sonnerup et al.*, 1981; *Scudder et al.*, 1981]. Bulk plasma flows in the magnetosheath were generally observed to be as predicted for slowing and deflection of the solar wind flow around the planetary obstacle. However, for some of the bow shock crossings by Voyager 1, the flow was observed to be slightly sunward; this was attributed to rapid expansions of the magnetosphere [*Siscoe et al.*, 1980; *Richardson*, 1987].

We describe the ion and electron observations made by the Ulysses solar wind plasma experiment in the Jovian magnetosheath in February 1992. Our focus will be on bulk plasma parameters such as density, temperature, and velocity. Individual plasma spectra will be shown in order to provide basic descriptions of boundary crossings, spectral shapes, and anisotropies, without providing detailed treatments of these topics. Plasma observations within the magnetosphere proper are the subject of a separate study [*Phillips et al.*, 1993]. We anticipate subsequent studies which will concentrate on the following subjects: (1) plasma heating at the bow shock; (2) boundary motions and overall magnetospheric configuration; (3) the magnetopause boundary layer; (4) anisotropies and waves.

TRAJECTORY AND INSTRUMENTATION

The Ulysses spacecraft was launched on October 6, 1990, and proceeded to Jupiter in order to obtain a gravitational assist to accomplish its primary mission of exploring the heliosphere at high heliographic latitudes. The inbound trajectory at Jupiter was similar to those of previous spacecraft, transiting the dawn, dayside magnetosheath and magnetosphere. The outbound trajectory was unique in that it transited the dusk, near-terminator sector. Previous spacecraft missions had established that the Jovian magnetosphere constitutes an obstacle which is relatively compressible when

Paper number 93JA02592.
0148-0227/93JA-02592$05.00

compared to its terrestrial counterpart. Thus it was no surprise that Ulysses encountered multiple crossings of the bow shock and magnetopause. A log of the plasma regimes observed by the plasma experiment has been published by *Bame et al.* [1992*b*]; we repeat this log, augmented by spacecraft position information and incorporating, a few minor changes and additional events, in Table 1. The first encounter with the bow shock occurred at 1733 UT on February 2, 1992, at a planetocentric distance of 113 Jupiter radii (R_J), Jovian local time of 1018, planetary latitude of +5°, and magnetic latitude of -4°. Closest approach to Jupiter was at 1202 UT on February 8, at 6.3 R_J and Jovian local time of 0130. The final encounter with the bow shock was at 0753 UT on February 16, at 149 R_J, Jovian local time of 1815, planetary latitude of -37°, and magnetic latitude of -28°.

The Ulysses solar wind plasma experiment comprises two separate sensors, one for electrons and one for positively charged ions; a complete instrument description was published by *Bame et al.* [1992*a*]. Both are spherical-section electrostatic analyzers which use channel electron multipliers (CEMs) to count particles discretely. The CEM arrays are aligned with the spacecraft axis so as to provide three-dimensional velocity space coverage, with the other two dimensions accounted for by vot tage stepping and spacecraft spin (five revolutions per minute). Both instruments were operated throughout the encounter, with the exception of a 24-hour shutdown near closest approach duc to increasing background counts and the goal of preserving CEM gains. Because the velocity distributions of electrons and ions in the solar wind arc markedly different, with beamlike ion fluxes and omnidirectional electron fluxes, the two instruments usc different approaches to accomplish the primary experimental goal of heliospheric science.

The electron instrument has an energy range of 1.6 to 862 eV in its usual mode and includes seven CEMs which, together with spacecraft spin, provide look angle coverage of 95% of 4π-steradians of solid angle. Each electron spectrum takes two minutes to measure. and includes 20 logarithmically spaced energy steps. During the Jupiter encounter the instrument was placed in a mode incorporating highest angular resolution, at a cost of decreased time resolution. Spectra were returned every 5.7 min, with two of every three spectra summed over the CEM array and returned as two-dimensional measurements. The angular step size in the spacecraft spin plane (normal to the Earth-spacecraft axis and nearly normal to the Sun-Jupiter axis during the encounter) was 5.625° (64 steps per spin) for two-dimensional spectra and 11.25° (32 steps per spin) for three-dimensional spectra, The instrument was configured with its maximum count integration time Of 64 ms to ensure maximum sensitivity during the encounter.

The ion instrument has an energy-per-charge (E/q) range of 248 eV/q to 12,2 keV/q for the measurements used in this study; the full instrumental range extends to 35.2 keV/q. Each spectrum includes 40 logarithmically-spaced E/q steps. In the solar wind, the ion energy peak is actively tracked so as to allow s% E/q spacing, over half of the logarithmic E/q range specified above, while still capturing the Complete proton and helium distributions, For the encounter, however, the active tracking, was disabled so as to return the full 248 eV/q to 12.2 keV/q range for the mode in usc, with 10% energy spacing, The instrument incorporates an aperture wheel to vary its sensitivity throughout its heliospheric mission; the largest aperture was selected for the encounter. Each ion spectrum takes 2 min (10 spacecraft spins, with four energies sampled per spin) to accumulate; during the encounter the spectrum repetition period was four minutes.

The ion analyzer includes an array of 16 CEMs, positioned so that the first CEM views along the spacecraft spin axis and the sixteenth views at a polar angle of 75° from the spin axis. Note that the spin axis points earthward; during the encounter this was approximately 5° from the sunward look direction. In order to accommodate the varying Sun-Earth-spacecraft geometry during the Ulysses mission and to adequately characterize the solar wind proton/alpha distributions within available telemetry limits, the ion analyzer returns data based on eleven predetermined arrays of CEM number and spin phase

TABLE 1. Summary of Entry Times, Exit Times, and Spacecraft Position, of Observed Plasma Regions

Transition	Boundary	Entry Date/ Time, UT		Exit Date/ Time, UT		Entry Distance (R_J)/ Latitude/Local Time			Exit Distance (R_J)/ Latitude/Local Time		
Msp-BL-Msh	BS	2/02	1733	?/02	1733	113	+05°	1018	113	+05°	1018
Msh-BL-Msh	MP[1]	2/0?	2130	2/02	2308	110	+05°	1018	109	+05°	1018
	MP[2]	2/02	2222	2/02	2308	109	+05	1018	109	+05	1018
Msp-BL-Msh	MP	2/03	1655	2/03	1720	096	+06"	1015	095	+06°	1015
Msh-BL-Msh	MP	2/03	1945	2/04	0025	093	+06°	1014	090	+06°	1013
Msh-BL-Msh	MP	2/04	0100	2/04	0125	090	+06°	1013	089	+06°	1013
Msh-BL-Msp	MP	2/04	0250	2/04	0400	088	+06°	1013	087	+06°	1012
Msp-BL-Msp		2/12	0024	2/12	0100	072	-36°	1839	073	-36°	1839
Msp-BL-Msp		2/12	1058	2/12	1226	080	-36"	835	082	-36°	1834
Msp-BL-Msh	MP	2/12	1337	2/12	1357	082	-36°	834	083	-36°	1834
Msh-BL-Msp	MP	2/12	1700	2/12	1740	085	-36°	833	085	-36°	1833
Msp-BL-Msh	MP	2/12	1820	2/12	1910	086	-36°	832	087	-36°	1832
Msh-SW	BS	2/14	0037	2/14	0037	t09	-37"	824	109	-37°	1824
SW-Msh	BS	2/14	0428	2/14	0428	112	-37"	824	112	-37°	1824
Msh-BL-Msp	MP	2/14	0933	2/14	1030	115	.37"	823	116	-37'	1822
Msp-BL-Msp		2/14	1400	2/14	1600	119	-37°	822	120	-37	1821
Msp-BL-Msp		2/14	1815	2/14	1825	122	-37"	1821	122	-37	1821
Msp-BL-Msh	MP	2/14	2045	2/1'1	2140	124	-37°	1820	124	-37"	1820
Msh-SW	BS	2/16	0753	2/16	07s3	149	-37°	1815	149	-37°	1815

Solar wind (SW), magnetosheath (Msh), boundary layer (Rl), and magnetosphere (Msp), with identification of the boundary crossed, bowshock (BS) or magnetopause (MP). [1]Based on magnetic field observations. [2]Based 011 plasma observations.

ombinations. The choice of measurement matrices is ommanded from the ground. During the encounter the easurement matrix and the spin-phase-indexed matrix center oint were selected based on the estimated flow direction for ach region. This scheme worked well for the outbound ncounter phase. During the inbound phase, which will be xplained in detail in a subsequent section, magnetosheath ion ea ents were stymied by (1) the unexpectedly early bow h ncounter; (2) the brief (4-hour) transit of the ag tosheath; (3) the anomalous flow orientation in the agnetosheath; and (4) the 75-min round-trip light time, hich precluded rapid response 10 unexpected plasma onditions. As a result, no meaningful ion measurements are vailable for the inbound magnetosheath encounter, except of ourse for standard solar wind measurements up until the first ow shock crossing.

Vector magnetic field measurements from the Ulysses ag eter experiment [*Balogh et al.*, 1992*a*] were used in r , the plasma observations throughout this study. Use f th se observations was primarily for (1) identification Of the ense (parallel or perpendicular) of anisotropies in electron istribution functions and (2) corroboration of the times of agnetopause crossings.

DATA REDUCTION ANI) LIMITATIONS

The omnidirectional character of the electron instrument its well for measurement not only of solar wind str as but also of magnetosheath and magnetospheric istributions, though its relatively low energy range is a miting factor in the magnetosphere. Reduction of the ectron measurements began with identification of the acecraft potential. This process, based on inflections in the ectra, is automated for routine solar wind measurements, but as carried out spectrum by spectrum for the Jupiter servations. Spacecraft potential is typically +4 to + 8 V in e solar wind, 42 to + 5 V in the magnetosheath, and higher sit values in the magnetosphere. Electrons measured at erg low $e\Phi$, where e is an electron charge and Φ is the acecraft potential, are photoelectrons electrostatically apped near the spacecraft. Electron count arrays were nverted to phase space density, arrays, corrected for acecraft potential, and numerically integrated to produce andard velocity-weighted moments: density, temperature mponents, and velocity vector.

The directional nature of the ion instrument, intended for perio solar wind characterization within telemetry ns is a moderate limitation when measuring agn th distributions and is a severe limitation in the agnetosphere. Data reduction consisted of conversion of unt arrays to phase space density arrays, followed by merical integration to produce similar moment products as f the electron instrument. In the solar wind tbc data reduction de splits the ion distributions into proton and alpha particle mponents. As will be explained later, the ion distributions the magnetosheath arc better characterized as the sum of ermal and suprathermal proton populations. Ion moments ttle this paper are thus based on a proton-alpha scheme r th ar wind, and a proton-proton scheme for the agnet sheath and magnetosphere.

The ion measurement matrices have angular extents which ample for characterization of the cold supersonic beams in solar wind. In the magnetosheath, even in the Supersonic region transited by Ulysses during the outbound phase of the encounter, the ion distributions are broad enough that they cannot be fully measured by the existing measurement matrices. In other words, the instrument still measures substantial count rates near the angular margins of its telemetered measurement space, whereas in the solar wind the countrates near the margins are zeroes. Additionally, the ion instrument aiming scheme, planned prior to the encounter based on expected sheath flow directions, had varying success in capturing the heart of the ion beam. While it is difficult to quantify the validity of the ion measurements, we can make the following statements about the magnetosheath ion moments produced by the numerical integration scheme. (1) Ion densities represent a moderate underestimate, typically by a factor of 2 when compared with the electron observations (which were validated by comparison with plasma-frequency derived densities, as discussed in a Subsequent section). During One interval of the outbound encounter (the first sheath interval on February 14; this interval will be discussed in more detail in a subsequent section) the pointing scheme clearly missed most of the beam, resulting in a density underestimate by a factor of 10 or greater. (2) Ion velocities are still reliable for most magnetosheath intervals. It is possible to estimate the bulk velocity of a cool, convecting population despite a restricted directional sampling of the. distribution function, as long as the heart of the distribution is measured (i.e., the bulk velocity vector lies within the measured velocity space). However, for the interval mentioned above in which the beam was not well - sampled, ttre velocities are unreliable, (3) Ion temperatures represent a substantial underestimate; the ions with the greatest velocity dispersion about the distribution centroid are those which are not observed. As will be shown in a subsequent section, fitting of individual spectra and comparison with Voyager results [*Richardson*, 1987] suggest that routine ion temperature calculations result in an underestimate by a factor of 2 to 10. We note that a similar limitation on sheath ion density determinations was discussed by *Intriligator and Wolfe* [1976] for the Pioneer 10 and 11 plasma analyzer. Comparison of the Pioneer sheath ion temperatures with those observed by Voyager 1 and 2 [*Richardson*, 1987], as well as with observations to be presented in this paper, suggests that the Pioneer temperature calculations were subject to an underestimation similar to that discussed above for Ulysses.

In presenting the data we will use a "Jupiter System III, solar longitude fixed" coordinate system. This system is Jupiter-centered, with **Z** northward along the planetary rotation axis. **X** is perpendicular to **Z** in the plane containing **Z** and the Sun-Jupiter line, positive antisunward. **Y** completes the right-handed set, positive dawnward. As Jupiter's rotation axis is offset from the normal to its orbital plane by only ~3°, this coordinate system is similar to the "RTN" system used by *Richardson* [1987].

INBOUND SHEATH TRANSIT

As previously noted, the inbound bow shock encounter occurred much earlier and much farther from the planet ($113 R_J$) than would be expected for nominal solar wind conditions. This is quite likely due to a decrease in solar wind plasma density, from a relatively normal ~0.2 cm^{-3} early on February 2, to ~0.02 - 0.08 cm^{-3} in the hours prior to the 1733 bow shock crossing [*Bame et al.*, 1992 *b*], though solar wind speed actually increased from ~450 to ~500 $km\ s^{-1}$ prior to the shock

encounter. Figure 1 (top panel) shows a sequence of spin- and orbit-averaged electron energy spectra in the solar wind and magnetosheath. The cool, two component (core plus halo) solar wind distribution, with temperature of 1.9×10^5 K (electron thermal speed $v_{te} = (kT_e/m_e)^{1/2} = 1696$ km s^{-1}) and density of 0.05 cm^{-3}, gives way to a hotter, denser ($T = 6.2 \times 10^5$ K, $n = 0.23$ cm^{-3}, $v_{te} = 3063$ km s^{-1}) distribution just inside the bow shock. This spectrum is followed by a less dense but much hotter ($T = 1.1 \times 10^6$ K, $n = 0.15$ cm^{-3}, $v_{te} = 4080$ km s^{-1}) spectrum at 1757 UT, after which the temperature decreases and the density remains steady ($T = 8.1 \times 10^5$ K, $n = 0.14$ cm^{-3}, $v_{te} = 3501$ km s^{-1} at 1849 UT). The characteristic flat-topped profile, as noted by *Montgomery et al.* [1970] for Earth and by *Scudder et al.* [1981] for Jupiter, is evident in all three sheath distributions in the energy range from ~18 eV (electron speed $v_e = (2kT_e/m_e)^{1/2} = 2500$ km s^{-1}) to 102 eV (6000 km s^{-1}).

The inbound magnetosheath crossing lasted only 4 hours or less, with the magnetic field rotating to a magnetospheric configuration at 2130 UT [*Balogh et al.*, 1992*b*], while the plasma electron measurements showed no clear evidence of a magnetospheric component until 2222 UT. After the plasma-based magnetopause crossing, the spacecraft entered a boundary layer, characterized by the presence of both "warm" electrons in the 10-100 eV range and a much hotter magnetospheric population (this boundary layer was visible in the ion observations as well during the outbound encounter phase). The sequence of electron spectra described above continues in the bottom panel of Figure 1, with an "inner sheath" spectrum measured 29 minutes prior to the field-based magnetopause crossing. Note the much cooler spectral slope in this distribution ($T = 3.7 \times 10^5$ K, $n = 0.17$ cm^{-3}, $v_{te} = 2366$ km s^{-1}), when compared to the sheath spectra in the top panel. After the field-based magnetopause determination, the overall electron distribution became less dense and still cooler ($T = 2.4 \times 10^5$ K, $n = 0.088$ cm^{-3}, $v_{te} = 1906$ km s^{-1} in the 2153 UT "sheath or BL" spectrum). After the plasma-based crossing, the distribution became hotter and still more rarefied as the lower-energy population disappeared and a magnetospheric population became evident ($T = 6.4 \times 10^5$ K, $n = 0.027$ cm^{-3}, $v_{te} = 3112$ km s^{-1} in the 2250 UT boundary layer spectrum). Finally, a purely magnetospheric spectrum ($T = 1.7 \times 10^6$ K, $n = 0.008$ cm^{-3}, $v_{te} = 5072$ km s^{-1}) was observed, nearly two hours after the field-based magnetopause crossing.

Figure 2 shows a time series of electron moments (n, T, and v) for the inbound shock, magnetosheath, and magnetopause crossing, as well as ion moments for the solar wind only. The solid trace represents three-dimensional electron spectra, dots show the two-dimensional electron results (for n and T only), and squares indicate ion measurements. The first two electron spectra after the shock crossing were two-dimensional spectra (two solid dots, with noticeably high density, including the postshock spectrum shown in Figure 1). Thus the solid trace marking the three-dimensional spectra in Figure 2 understates the density enhancement at the shock. Note that the evidence for a planetary depletion layer (i.e., a decrease in density outside the magnetopause) depends in part on whether one adopts the 2130 UT or the 2222 UT magnetopause determination [cf., *Hammond et al.*, 1993]. Note also that the sheath electron temperature decreases steadily, with the exception of an increasing trend from 1920 to 2000 UT throughout the sheath transit. A similar, though less severe, overall temperature decline was observed by Voyager 1 [*Scudder et al.*, 1981]. We will discuss the subject of electron heating in a subsequent section on the outbound encounter phase. Note, however, that the electron heating at the Earth bow shock has been demonstrated [*Thomsen et al.*, 1987] to depend on the solar wind flow speed in the shock frame and that a decrease in electron temperature from the bow shock to the magnetopause may be interpreted as a manifestation of decreasing solar wind speed in that frame, rather than as a spatial feature.

The electron bulk velocity in the sheath shows a dramatic trend, reminiscent of that seen during the Voyager 1 encounter [*Siscoe et al.*, 1980; *Richardson*, 1987]. While V_Y remains positive throughout the sheath, as appropriate for a dawn-side transit, and V_Z is variable and relatively small in magnitude, as expected for the low latitude sheath, V_X reverses from positive (antisunward) in the outer sheath to negative (sunward) in the inner sheath and boundary layer. This is further evidence for expansion of the magnetosphere, which resulted in an anomalous shock position and rapid transit of the magnetosheath. Note the temperature peak in the middle magnetosheath (near 1930 UT), which is roughly concurrent with the reversal in V_X; it is unclear whether this peak is related to the boundary between inward and outward flows.

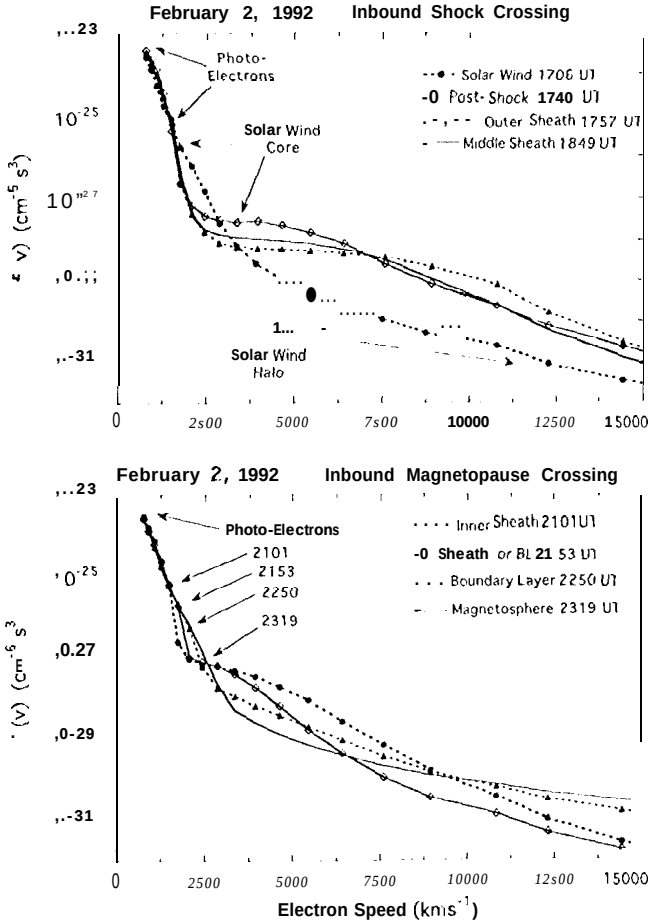

Fig. 1. Sample one-dimensionalized electron spectra for the initial (top) inbound bow shock crossing and (bottom) magnetopause crowing. Magnetosheath spectra are shown in both panels. In the top panel the energy range dominated by spacecraft photoelectrons was roughly the same for all spectra and is marked in the figure. In the bottom panel the photoelectron range varied among spectra; the top of this range is marked for each plotted spectrum.

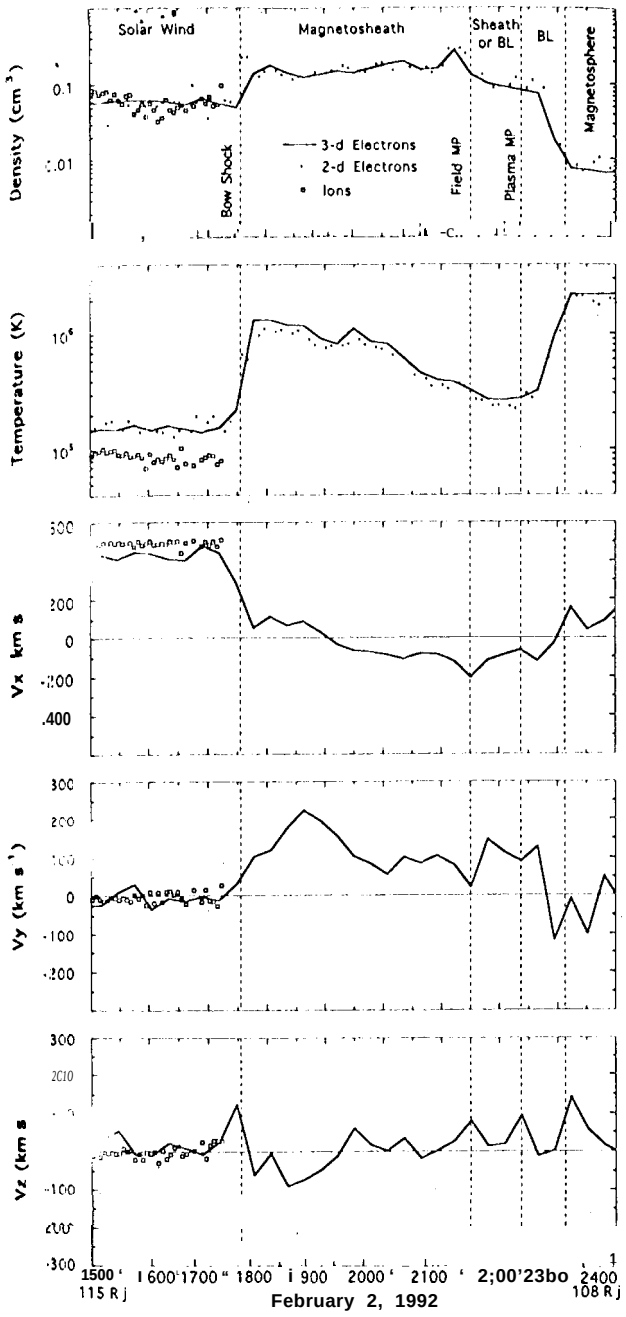

'4 2. 'rime series of plasma density (panel 1), temperature (panel 2), ed velocity (Jupiter System III, solar longitude fixed; see **description in** ut panels 3-5) for 1500 to 2400 UT **on February 2, 1993. This** interval : otain itial **inbound bow shock and** magnetopause **encounters.** The leg op panel) shows the **symbols for three-dimensional** lectron, two-dimensional electron, **and** ion observations. Ion data are ailable only for the solar wind, for **reasons** described in the **text.**

Later in its inbound passage, Ulysses reencountered the agnetopause boundary layer and magnetosheath. As shown n Table 1, these encounters included a magnetopause crossing uring the period 1655 to 1720 UT on February 3 (day 34), ollowed immediately by an excursion back into the boundary ayer at UT. The boundary layer transit continued until 1925 U the following day, when the spacecraft again assed briefly int the magnetosheath and then back through he boundary layer and into the magnetosphere at 0400 UT. ndividual spectra from this prolonged, glancing nCounter with the magnetosheath and boundary layer will not be examined in detail here. However, Figure 3 shows the electron moments, in the same format as Figure 2. Note that the electron temperature in the sheath is much higher (-6x 10^5 K) during this interval than during the initial inbound sheath transit, Perhaps the most striking feature in Figure 3 is the lack of antisunward flow (V_X), suggesting that the magnetopause normal is nearly sunward. The two sheath intervals, with a local time range of 1013 to 1015 and planetary latitude of +6°, are characterized by dawnward and southward flow (though the flow in the adjacent boundary layers is northward). Note also that the sheath plasma density tends to be low near the magnetopause (i.e., just outside the

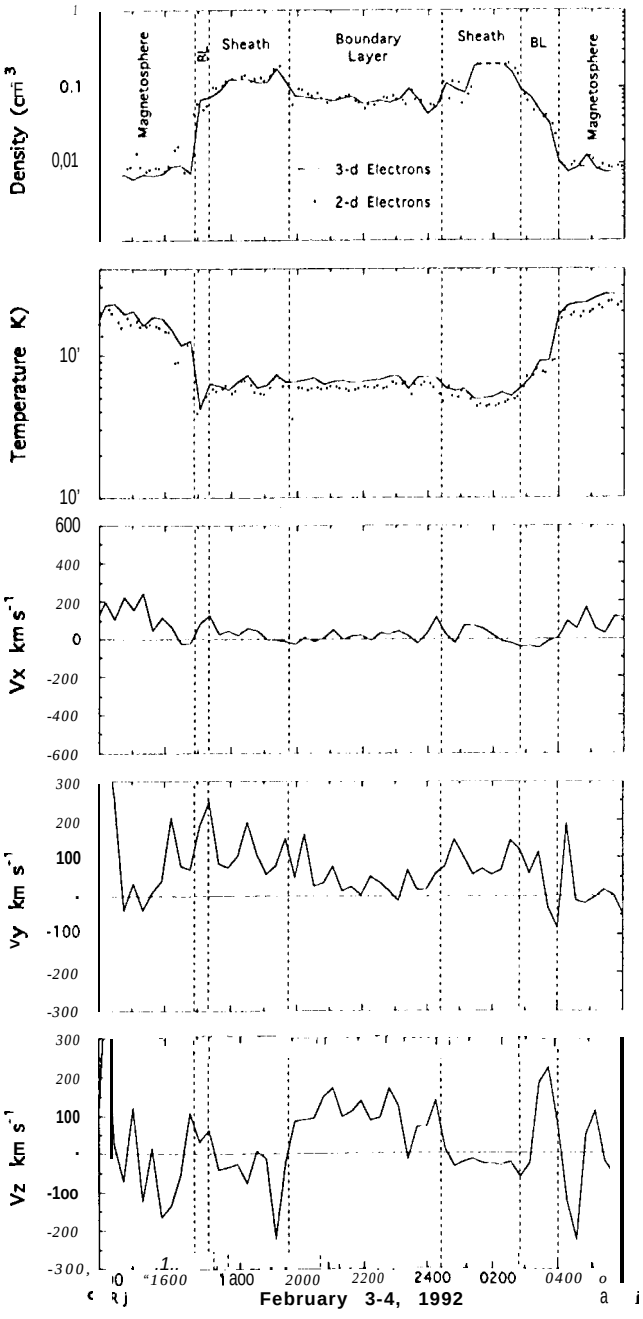

Fig. 3. Time series, in the same format as Figure 2, for electron data only, for 1400 UT on February 3 through 0600 UT on February 4. This **interval contains a glancing encounter with the** magnetopause **boundary layer and** magnetosheath.

boundary layer) for all four magnetopause crossings shown in Figure 3, suggesting the existence of a planetary depletion layer [et'., *Hammond et al.*, *1993]. Wc* anticipate further analysis of this interval in subsequent studies on boundary motions and the magnetopause boundary layer.

OUTBOUND SHEATH TRANSIT

The outbound transit of the Jovian environment by Ulysses was characterized by multiple boundary crossings, as listed in Table 1. During this phase of the encounter the ion instrument was configured to make valuable magnetosheath measurements, subject to the instrumental limitations described previously. The ion observations in the magnetosphere and boundary layer arc perhaps of less validity but will be included here for completeness. Plate 1 summarizes the outbound encounter phase from 1200 UT on February 12 (day 43) through 1200 UT on February 16 (day 47). In this color-coded spectrogram, each 24-boor interval is represented by a pair of panels, one for ions (top) and onc for electrons (bottom); day of year is indicated at the lower left corner of each pair of panels. Each panel represents a counts-versus-energy spectrum, summed over all measured look directions, for the available energy range of each instrument. The legend at right shows tbc color table for each species. In the electron panels the dark band at the bottom represents two unused 10 W-energy steps, and the red band just above it represents photoelectrons trapped by the positive spacecraft potential. White vertical bands arc data gaps, and the occasional count enhancements at high energies (0810 and 0910 UT on day 44; 0715 UT on day 45) are spurious.

In the solar wind (early on day 45, plus the last observations on day 47) the electron counts are predominantly at low energies, while the ion spectra show distinct proton and alpha particle beams (the abrupt switch-on of these beams at 0225 UT on day 45 resulted from a commanded configuration change which brought the solar wind into the field of view). In the magnetosheath (for example, 1910 UT on day 43 through the end of day 44, and 2140 UT on day 45 through 0800 UT on day 47), both ion and electron instruments show' high count rates, near 1 keV (ions) and tens of CV (electrons). In the magnetosphere (for example, 1100-1200 UT on day 45) tbc electron spectra show a distinct population at highest measured energies, while the ion spectra are nearly featureless. For this interval, note that the red band near 5 eV, which fades to yellow near 10 eV, represents trapped photoelectrons, not ambient electrons. The ambient electrons appear as the light blue region at ~100 eV or greater. The red-yellow region extends to higher energies here than during the sheath intervals, because the ambient electron density is lower and the spacecraft potential is higher. The boundary layer (for example, 1820 to 1910 UT on day 43) has characteristics of both magnetosheath and magnetospheric spectra.

Figure 4 (top panel) shows one-dimensionalized electron spectra for the double shock crossing early on February 14 (day 45; shock crossings at 0037 and 0428 UT). The solar wind core (thermal) distribution was quite cold during this interval; the depicted spectrum has a temperature of about 2.0×10^4 K. The breakpoint between photoelectrons and ambient thermal electrons is invisible in this presentation but was noticeable in other display formats used to make the breakpoint identification, The spectral range identified as core electrons is marked by a solid bar in the figure. The slight inflection in the solar wind spectrum near 4000-7000 km s^{-1} (45-139 eV) represents an enhanced suprathermal heat flux originating at the shock, This flux is very localized in angle, and is largely Washed out by the angle averaging done for Figure 4. Note that the preshock magnetosheath spectrum (0000 UT) is much cooler and much denser ($T = 1.3 \times 10^5$ K, $n = 3.8$ cm^{-3}, v_{te} = [404 km s^{-1}, than the post-shock (0451 UT) spectrum ($T = 1.1 \times 10^5$ K, $n = 1.1$ cm^{-3}, $v_{te} = 2462$ km s^{-1}).

Figure 4 (bottom panel) shows a similar sequence of spectra for the sheath-boorrdary layer-magnetosphere crossing which occurred a fcw hours later (magnetopause crossing at 0933 UT, boundary layer exit at 1030 UT). The first two spectra are from the magnetosheath. Note that the.rc is a marked downward trend in both temperature and density from the 045 I UT outer sheath spectrum (top panel), to the 0628 UT middle sheath spectrum ($T = 3.6 \times 10^5$ K, n = 0.64 cm^{-3}, v_{te} = 2336 km S-l)), to the 0830 UT inner sheath spectrum (7' = 2.7 x 105 K, n = 0.3 c'"$^{-3}$, v_{te} = 2023 km s^{-1}). In the boundary layer spectrum, the cooling trend continues at lower energies, and an additional low component is visible, The low total electron temperature (0939 UT; $T = 8.0 \times 10^4$ K, n = 0.69 en^{-3}, v_{te} = 1101 km s^{-1}) suggests that the cooling of the sheath component has not been overcome by the addition of the hot magnetospheric population. Finally, in the magnetospheric spectrum (1 UT; 7'= 1.3 x 10^6 K, n = 0.015 cm^{-3}, v_{te} = 4439 km S-l) low-energy component has vanished.

The magnetosheath ion spectra for the outbound encounter phase support the Voyager 1 findings of *Richardson* [19 namely the existence of a two-component proton population. Figure 5 contains two spectral cuts (solid dots), roughly along the velocity vector, for spectra observed in the inner sheath (top panel) and outer sheath (bottom). The dashed traces are fits to thermal and suprathermal Maxwellians convecting at the same speed; the convection speed and the fit temperatures and densities arc shown in the figure. The solid trace represents the sum of the two fits for each panel. In some spectra (not shown here) a slight inflection near twice the energy pcr charge of the proton peak, presumably due to He^{++}, is also observable. The densities and temperatures of the thermal and suprathermal components in the plotted spectra arc within the ranges observed by Voyager 1. Note that these one-dimensional moments produce densities and temperatures substantially higher than those calculated with routine numerical integration of the observable part of the distribution functions. For example, the spectrum in the top panel of Figure s, if assumed to be isotropic, yields a total density of 0,70 cm^{-3} and a thermal temperature of 2.3×10^6 K, whereas the integrated moments produce n = 0.34 cm^{-3} and $T = 5{,}7 \times 10^5$ K, This supports the earlier subjective statement that the numerical ion moments can bc considered to bc underestimates of density and may be serious underestimates of temperature. The suprathermal proton component is also observed in the terrestrial magnetosheath [c. g., *Sckopke et al.* , 1983] and can be attributed to the reflection of the incident solar wind ions at the bow shock, followed by their gyration and convection back through the shock [e.g., *Thomsen and Gosling*, 1 *Gosling and Robson*, 1985]. wc note that the shock configuration was observed to bc nearly perpendicular at both outbound crossings [*Balogh et al.*, 1992 *b*]; this geometry enhances the efficiency of the ion gyration/convection process.

Notwithstanding the above discussed limitations of the instrument and data reduction, wc include the numeric

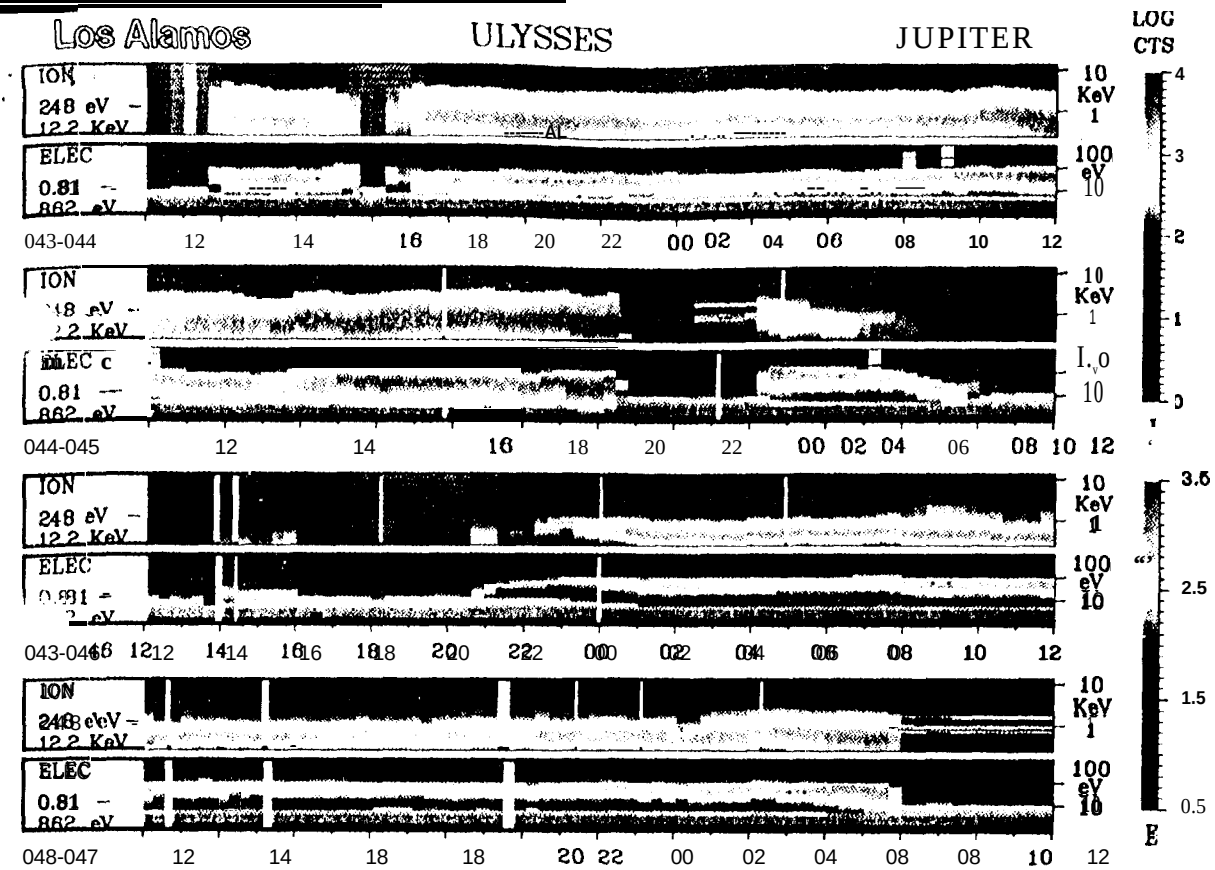

Plate 1. Color-coded ion and electron spectrogram for part of the outer encounter phase, including all boundary crossings and magnetosheath transits. Each pair of panels (ion and electron) spans a 24-hour period starting at 1200 UT; the day-of-year range for each panel pair is shown just below the left margin of each pair. The full ion proton-alpha particle energy range and the full electron energy range reshown. Ion and electron color tables, corresponding to angle-averaged counts, arc shown at right.

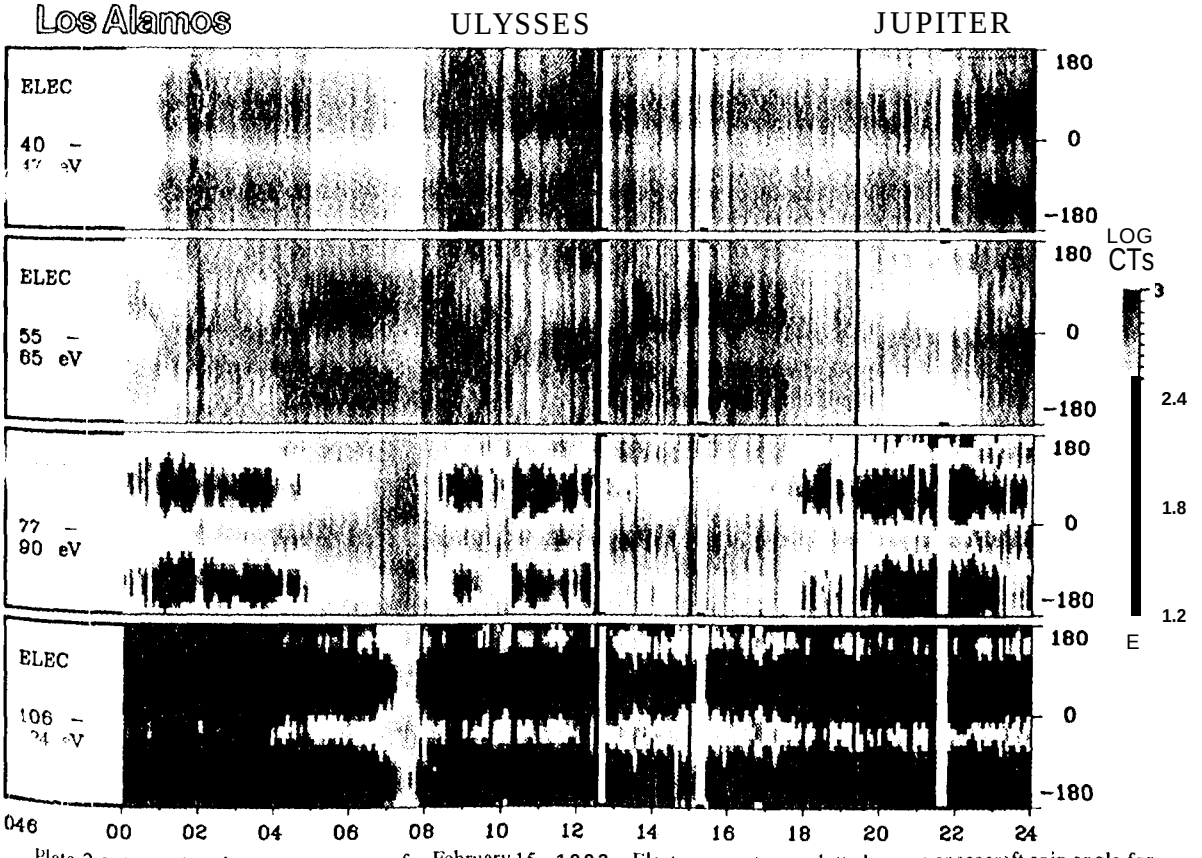

Plate 2 Color-coded electron spectrogram for February 15, 1993, Electron counts are plotted versus spacecraft spin angle for four energy ranges, indicated at the left border of each panel. Color table is shown at right. The ±B direction during this interval, corresponding to the angles shown at the right border of each panel, averages +65°/-115°.

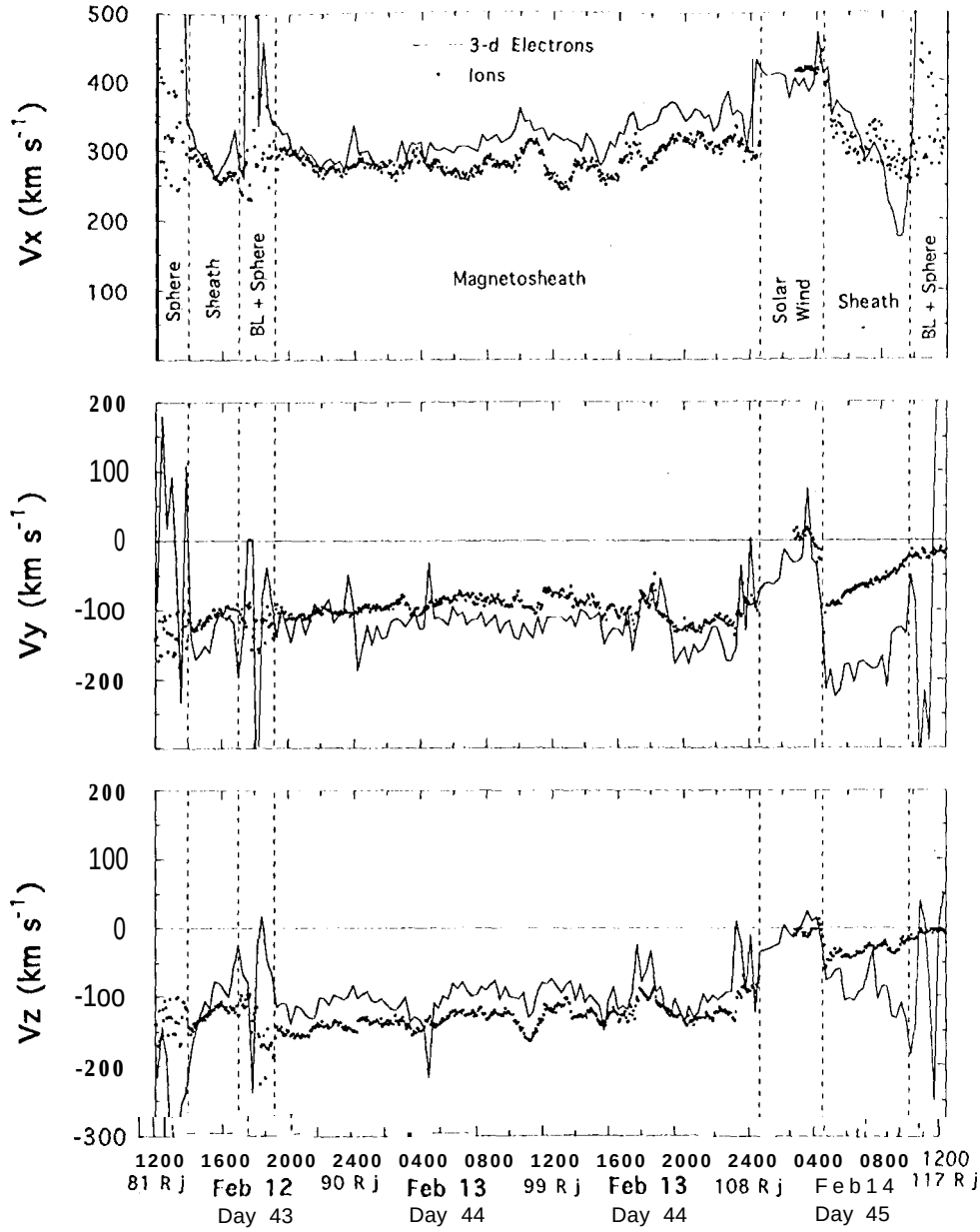

Fig. 7. Time series of ion and three-dimensional **electron velocity (Jupiter** System III, solar **longitude fixed;** see **description in text) for the period corresponding to the top half of** Plate **1:1200 UT on February 12 through 1200 UT** on February 14.

For the first sheath transit of the inbound encounter phase (Figure 2) we had noted that the electron temperature declined as the spacecraft moved from the bow shock to the magnetopause. This trend did not recur for the sheath transit and outward bow shock crossing of February 12-13 (Figure 6), but was obvious in the subsequent inward bow shock crossing and sheath transit of February 14 (Figure 6). For the final sheath transit and outward bow shock crossing (February 14-16; Figure 8), the temperature gradient was actually reversed near the shock, as noted in the preceding paragraph. Additionally, we had noted that the plasma density was considerably higher before the outward shock crossing on February 13 (Figure 6) than after the inward shock crossing a few hours later. We suggest that these features support the findings of *Thomsen et al.* [1 987] that electron heating is largely controlled by flow speed, specifically by the upstream flow speed in the shock frame. The compressibility of the Jovian magnetosphere, and the occurrence of rapid boundary motions, suggests that motions can dominate the overall configuration o magnetosheath, and that features which might be interpret spatial are more likely to be manifestations of tem changes. We have examined the plasma observations for of ISEE 2 transits of the terrestrial magnetosheath and found no consistent trend in temperature from the bow sh the magnetopause. We suggest the following scenario f Ulysses observations at Jupiter. Both inward (solar wi magnetosheath) shock crossings (February 3 ancl Februar occurred during periods of magnetospheric expansion, the outward crossings occurred during interva magnetospheric contraction or stability. This is suppor the observations of high sheath densities just inside th shock prior to both outward crossings; these high densiti presumably due to high solar wind densities. which course result in compression of the magnetosphere an

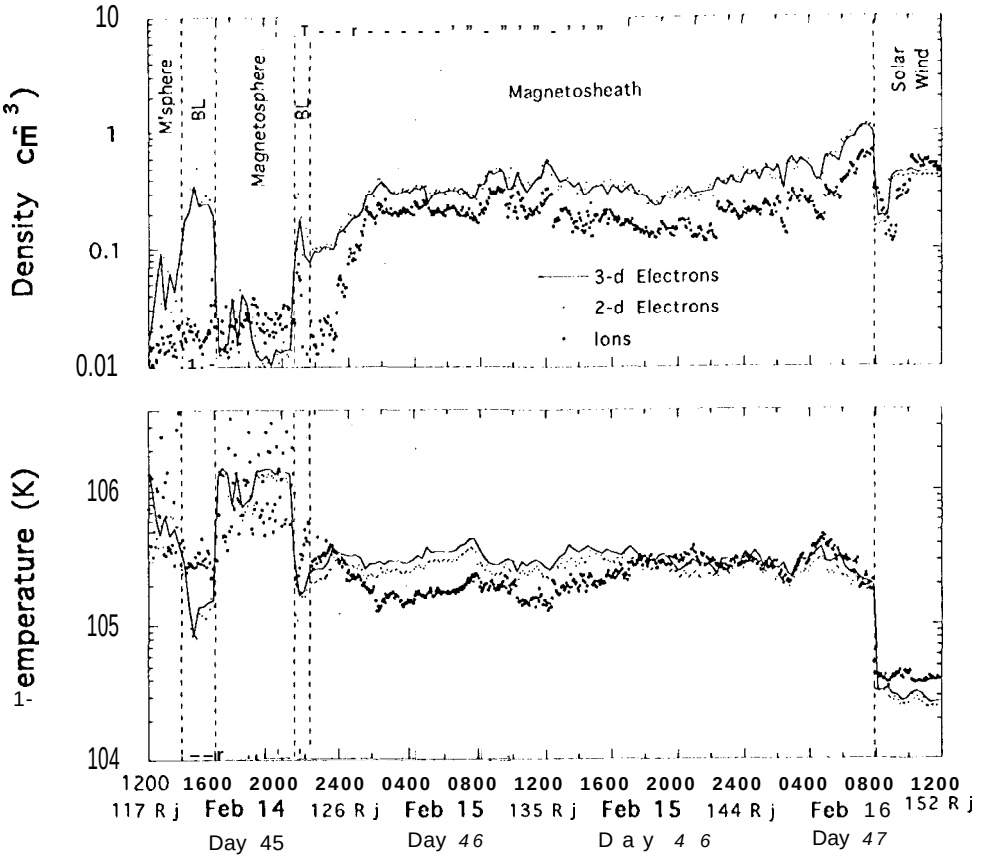

Fig. 8. Same format as Figure 6, but for the interval corresponding to the bottom half of Plate 1: 1200 UT on February 14 through 1200 UT on February 16.

of the bow shock. An expanding shock (inward crossings) results in high upstream flow speed in the shock frame and thus in enhanced electron heating, while a contracting shock (outward wings) has the opposite effect. We intend to quantify this analysis in a subsequent study.

Figure 9 continues the presentation of bulk plasma parameters, showing ion and electron velocity vectors for the same interval as in Figure 8. Once again, the calculated ion and electron velocities in the sheath agree reasonably well. The overall sheath velocities are again unremarkable, with speeds in the 300 - 400 km s^{-1} range and an antisunward, duskward, and southward orientation. The flow can be seen to be most nearly antisunward near the bow shock, and more strongly duskward - the magnetopause. As in the previous 48-hour interval, ion velocities in the magnetosphere are highly variable but are most nearly antisunward, with speeds often exceeding 1000 km s^{-1}, while velocities in the boundary layer appear to be a combination of the magnetosheath and magnetospheric components.

The final observational topic we will present concerns electron anisotropies. While further work remains to be done on analysis of both the ion and electron distribution shapes, it is clear that systematic anisotropies exist. Plate 2 is a 24-hour color-coded spectrogram of electron count rates in four different energy ranges, plotted against spacecraft spin angle, for February 15 (day 46). The magnetic field during this interval was generally within 30° of the spin plane, with a ±B orientation averaging 65°/-115° when projected onto that plane. Note in the top panel (40-47 eV) of Plate 2 that the peak electron counts were generally observed in the field-aligned spin phases. In the two lowest panels (77-90 eV and 106-124 eV), however, the peak count sectors are clearly aligned perpendicular to B. In the second panel (55-65 eV) the spin angles corresponding to peak electron counts are sometimes field-aligned and sometimes perpendicular to B. Anisotropic electron fluxes of this type are observable in all the outbound magnetosheath intervals, but most strongly during the final sheath transit on February 15 and 16.

Figure 10 displays a representative electron spectrum from this interval, measured at 0329 UT on February 15. The top panel shows phase space density vs. electron speed in two cuts, one nearly parallel and one nearly perpendicular to B. Note the pronounced flat top in the parallel cut at thermal energies (18 to 45 eV, v_e = 2500 to 4000 km S-l). Parallel phase space density, $f(v_{\parallel})$, exceeds $f(v_{\perp})$ at energies below 45 eV, while $f(v_{\perp})$ is dominant at higher energies, The lower panel shows another view of the same spectrum, this time with $f(\mathbf{v})$ plotted vs. spacecraft spin angle at six thermal and suprathermal energies. The ±B direction is marked by vertical traces. The flat-topped nature of the distribution is evident in the constancy of $f(\mathbf{v})$ at thermal energies (23, 32, and 44 eV), particularly in the direction parallel to the magnetic field. Note once again that the sense of the anisotropy (field-aligned or transverse) reverses between 44 and 61 eV. Similar electron signatures have been observed in the terrestrial magnetosheath [e.g., *Feldman et al.*, 1983; Gosling *et al.*, 1989] and attributed to complex processes arising from both microscopic and macroscopic features of the bow shock.

The overall effect of the electron anisotropies is that $T_{\perp}$ generally exceeds $T_{\parallel}$ by a factor of 1.2 to 2 throughout the

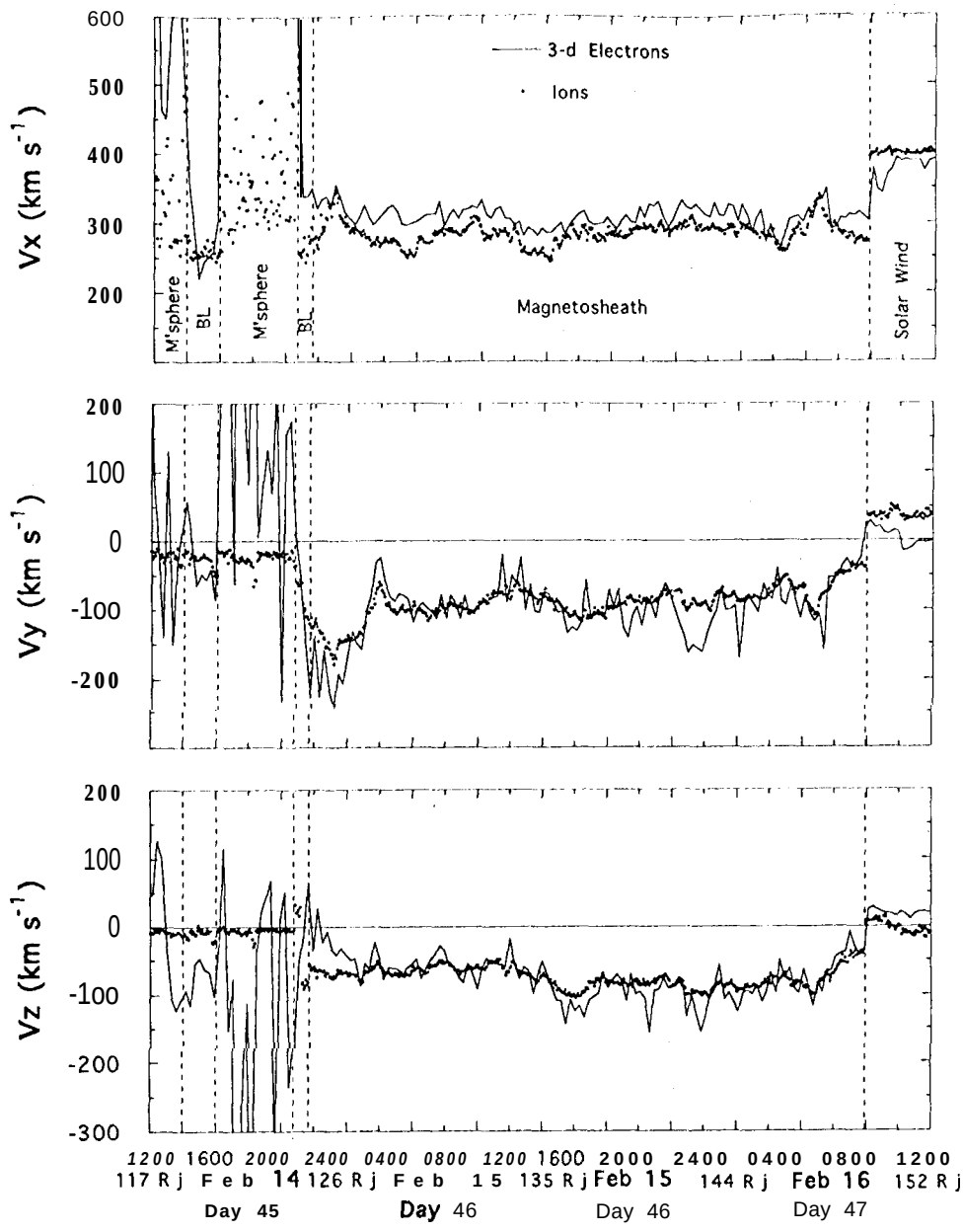

Fig. 9. Same format as Figure 7, but **for the interval corresponding to the bottom half of Plate 1: 1200** UT on February 14 through 1200 UT on February 16.

magnetosheath. Although detailed characterization of the magnetosheath ion distributions remains to be done, it appears that the ions have anisotropies of similar magnitude and sense. Such anisotropies are conducive to the growth of both ion cyclotron and mirror instabilities, and field signatures suggestive of these modes have indeed been observed in the Jovian magnetosheath [*Balogh et al., 1992b; Tsurutani et al.,* this issue], We note that the growth of these wave modes is sensitive to the relative abundances and anisotropies of both helium ions and suprathermal protons [e.g., *Gary et al.*, 1993]. Thus a careful analysis of both magnetic field and plasma data in the magnetosheath is necessary for full understanding of the wave modes and free energy sources present.

While the focus of the present study is on the magnetosheath, and not the magnetopause boundary layer, we note that the electron anisotropies within the boundary layer have the sense of $f(v_{||}) > f(v_{\perp})$. These anisotropies prevail for all boundary layer encounters, for both the low- (sheathlike) and high-energy (magnetospheric) compo Detailed work in separation of the two electron popul and quantification of the anisotropies, remains to be do present, however, it appears that the overall anisotro the **boundary layer electrons typically result in** $T_{||}$ **-1.5 the measured** energy range, Anisotropies of this sens been observed in the terrestrial boundary layer [e.g., *et al.*, 1984] and used to argue in favor of closed ma topology,

SUMMARY

During February 1992, Ulysses transited the Jovian environment, The solar wind plasma experiment reti unique set of ion and electron measurements magnetosphere, magnetosheath, and magnetopause bo

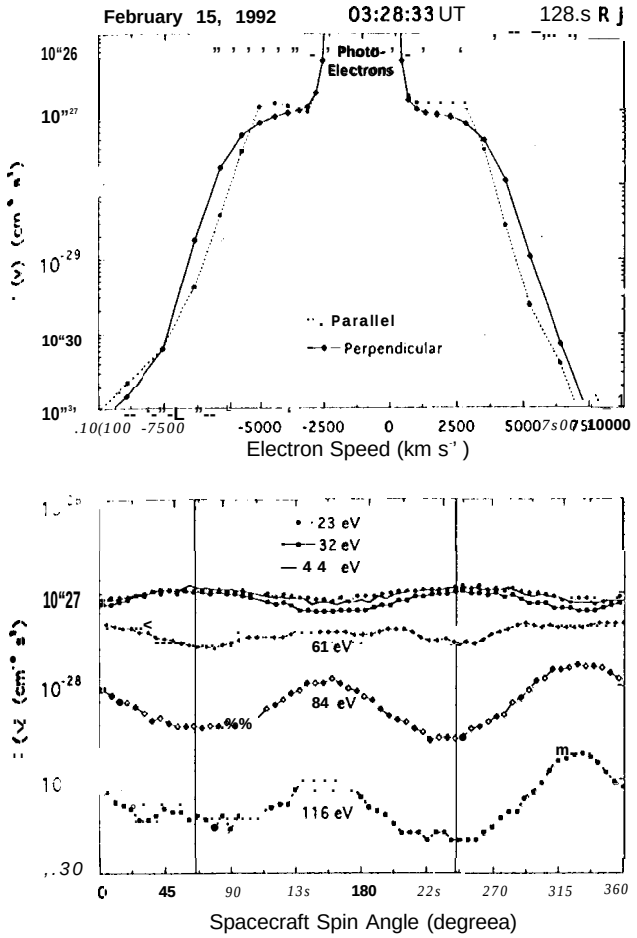

Fig. 10. **Single electron spectrum from the magnetosheath, measured at 128.5 Jupiter radii at 0328 UT on February 15. (Top) Cuts through the distribution function, roughly parallel (dashed trace) and perpendicular (solid trace) to the observed magnetic field. (Bottom) Phase space density as a function of spacecraft spin angle for six energy ranges. Plus/minus magnetic field direction is marked by vertical traces,**

layer. **Subject to the, inherent limitations of solar** wind instruments in a planetary environment, the instruments performed flawlessly. During the inbound encounter phase, Ulysses made a rapid transit of the low-latitude, dawnside magnetosheath during an interval of magnetospheric expansion, followed ~24 hours later by a prolonged, glancing encounter with the magnetosheath **and boundary layer. During the outbound phase the spacecraft encountered the** midlatitude, duskside magnetosheath four separate times and made three bow shock **crossings,**

Notable plasma features and trends include the following: (1) Magnetosheath electron temperatures were elevated during the two inward bow shock crossings but not during the two outward Crossings (2) Electron temperatures were generally in the range of 2 to 6 × 10^5 K within the magnetosheath. (3) Ion and electron densities and flow velocities during the sheath interval in the outbound encounter phase were generally as expected, slowing and diversion of the solar wind flow around the magnetospheric obstacle. (4) During the inbound encounter phase the first sheath transit occurred during a period of magnetospheric expansion, resulting in sunward plasma flow near the magnetopause. (5) During the subsequent glancing sheath encounter, the flow was predominantly downward, suggesting that the magnetopause **boundary** normal **was nearly** sunward. **(6)** Each magnetopause **crossing** showed evidence for a boundary layer, with coexisting sheathlike and magnetospheric electron populations; similar signatures were observed in the ion measurements during the outbound encounter phase. (7) Ion distributions in the sheath during the **outbound** encounter arc **best characterized as the** sum of thermal and suprathermal proton distributions. (8) Electron distributions in the magnetosheath arc flat-topped, with $f(v_{\|}) > f(v_{\perp})$ at thermal energies and $f(v_{\perp})$ **dominant** at higher energies. (9) Ion and electron anisotropies have the sense of $T_{\perp} > T_{\|}$, suggesting conditions conducive to the growth of the mirror mode and ion cyclotron instabilities.

The magnetosheath observations by the Ulysses plasma experiment confirm, and often elucidate in greater detail, prior discoveries by the Pioneer and Voyager experimenters. While there are some unique new results, such as the electron anisotropies, there arc no ncw findings which directly contradict previous understanding. The existence of sunward flow in the magnetosheath is further confirmation of the compressibility of the obstacle [e.g., *Siscoe et al.*, 1980]. The magnetopause boundary layer, previously recognized by *Sonnerup et al. [1981]* and *Scudder et al.* [1981], was observed at all magnetopause crossings. Ion and electron temperatures arc generally consistent with those previously reported, subject of course to the limitations of the measurements and data analysis, The observation of a substantial suprathermal proton population in the magnetosheath supports the findings of *Richardson [1987].*

Onc general characteristic of the magnetosheath of Jupiter is that it is remarkably similar to its terrestrial counterpart. With the exception of the rapid boundary motion and generation of anomalous sheath flows due to the compressibility of the Jovian magnetosphere, plasma characteristics observed by Ulysses in **the** magnetosheath of Jupiter match those seen in Earth's magnetosheath by various spacecraft, These characteristics, including electron distribution shapes, the presence of a suprathermal proton component, ancl the trends in electron heating at the shock, are reasonably well understood in terms of shock physics and dynamics. 'J'he presence of a magnetopause boundary layer, with coexisting plasma populations of solar and magnetospheric origin, invites further analysis of the mechanisms for crossing of the magnetopause by solar plasma, We note in passing that evidence suggests that the interplanetary magnetic field generally had a southward component throughout the encounter, an orientation not expected to be conducive for reconnection with the southward planetary field,

This study has taken the form of a "guided tour" of the Ulysses observations in the Jovian magnetosheath. We have attempted to be complete, in the sense of showing all the data for the reader's examination, Detailed topical analysis will be presented in subsequent studies, We anticipate further work on the boundary layer, **sheath** anisotropies **and** waves, shock heating, and boundary motions, as well as on plasma characteristics of the magnetosphere itself,

Acknowledgments. **We gratefully acknowledge the support of the Ulysses project, operations, and data management teams from JPL and** ESA. **Jupiter encounter planning, instrument operations, and subsequent data reduction and analysis involved contributions from many members of the Ulysses** plasma **experiment team,** including B. L. Barraclough, G. L. Gisler, J, T. Gosling, S. J. Kedge, D J. McComas, and K. J. Sofaly (LANL), M. Neugebauer **and R,** Sakurai (JPL), **and J. C. Chavez** (Sandia

National Laboratories). We thank A. Balogh and R. J, Forsyth for providing magnetometer data, and P. Canu, P. J. Kellogg, and R. G. Stone for providing density observations from the Unified Radio turd Plasma Wave experiment. We appreciate helpful suggestions by W. C. Feldman, C. M. Hammond, S. P. Gary, G. L. Siscoe, and the two referees. A portion of the work reported here was carried out by the Jet Propulsion Laboratory, California Institute of Technology, under a contract with the National Aeronautics and Space Administration, Work at Los Alamos was carried out under the auspices of the U.S. Department of Energy with financial support from NASA.

The Editor thanks G. Paschmann and another referee for their assistance in evaluating this paper.

REFERENCES

Balogh, A., T. J. Beck, R. J. Forsyth, P. C. Hedgecock, R. J. Marquedant, E. J. Smith, D. J. Southwood, and B. T. Tsurutani, The magnetic field investigation on the Ulvsses mission: Instrumentation and preliminary scientific results, *Astron. Astrophys. Suppl. Ser.*, *92*, 221, 1992*a*.

Balogh, A., M. K. Dougherty, R. J. Forsyth, D. J. Southwood, E. J. Smith, B. T. Tsurutani, N. Murphy, and M. E. Burton, Magnetic field observations during the Ulysses flyby of Jupiter, *Science*, 257, 1515, 1992*b*.

Bame, S. J., D. J. McComas, B. L. Barraclough, J. L. Phillips, K. J. Sofaly, J. C. Chavez. B. E, Goldstein, and R. K. Sakurai, The Ulysses solar wind plasma experiment, *Astron. Astrophys. Suppl. Ser.*, 92, 237, 1992rr.

Bame, S. J., et al., Jupiter's magnetosphere: Plasma description from the Ulysses flyby, *Science, 257, 1539,* 1992*b*.

Feldman, W. C., R. C. Anderson, S. J. Bame, S. P. Gary, J. T. Gosling, D. J. McComas, M. F. Thomsen, G. Paschmann, and M. M. Hoppe, Electron velocity distributions near the Earth's bow shock, *J. Geophys. Res.*, *88*, 96, 1983.

Gary, S. P., B. J. Anderson, R. E. Denton, S. A. Fuselier, M. E. McKean, and D. Winske, Ion anisotropies in the magnetosheath, *Geophys. Res. Lett.*, 20, 1767, 1993.

Gosling, J. T., and A. E. Robson, Ion reflection, gyration, and dissipation at super-critical shocks, in *Collisionless Shocks in the Heliosphere: Reviews of Current Research, Geophys. Monogr. Ser.*, vol. 35, edited by B. T. Tsurutani and R. G. Stone, p. 141, AGU, Washington, D. C., 1985.

Gosling, J. T., M. F. Thomsen, S. J. Bame, and C. T. Russell, Suprathermal electrons at Earth's bow shock, J, *Geophys. Res.*, *94*, *10,011,1989.*

Hammond, C. M., J. L. Phillips, S. J. Bame, E. J. Smith, and C. G. Maclennan, Ulysses observations of the planetary depiction layer at Jupiter, *Planet. Space Sci., in* press, 1993.

Intriligator, D. S., and J. H. Wolfe, Results of the plasma analyzer experiment on Pioneers 10 and 11, in *Jupiter*, edited by T. Gehrels, p. 848, University of Arizona, Tucson, 1976.

Montgomery, M. D., J. R. Asbridge, and S. J. Borne, VELA 4 plasma measurements near the Earth's bow shock, *J. Geophys. Res.*, 75, 1217, 1970.

Ogilvie, K. W., R. J. Fitzenreiter, and J. D. Scudder, Observation of electron beams in the tow-latitude boundary layer, *J. Geophys. Res.*, 89, 10,723, 1984,

Phillips, J. L., S. J. Bame, B. L. Barraclough, D. J. McComas, R. J. Forsyth, P. Canu, and P, J, Kellogg, Ulysses Plasma Electron Observations in the Jovian Magnetosphere, *Planet. Space Sci.*, in press, 1993.

Richardson, J. D., Ion distributions in the dayside magnetosheaths of Jupiter and Saturn, J. *Geophys. Res.*, *92*, 6133, 1987.

Sckopke, N., G. Paschmann, S. J. Bame, J. T. Gosling, and C. T. Russell, Evolution of ion distributions across the nearly perpendicular bow shock: Specularly and nonspecularly reflected ions, *J. Geophys. Res.*, 88.6121, 1983.

Scudder, J. D., E. C. Sittler, Jr., and H. S. Bridge. A survey of the plasma electron environment of Jupiter: A view from Voyager, *J. Geophys. Res.*, 86.8157, 1981.

Siscoe, G. L., N". U. Crooker, and J. W. Belcher, Sunward flow in Jupiter's magnetosheath, *Geophys. Res. Lett.*, 7,25, 1980.

Sonnerup, B. U. O., E. J. Smith, B. T. Tsurutani, and J. H. Wolfe, Structure of Jupiter' s magnetopause: Pioneer 10 and 11 observations, *J. Geophys. Res.*, 86, 332t, 1981.

Thomsen, M. F., and J. T. Gosling, Comment on "Ion distributions in the dayside magnetosheaths of Jupiter and Saturn" by J. D. Richardson, *J. Geophys. Res.*, *93*, 2761, 1988.

Thomsen, M. F., M. M. Mellott, J. A. Stansberry, S. J. Bame, J. T. Gosling, and C. T. Russell, Strong electron heating at the Earth's bow shock, *J. Geophys. Res.*, *92*, *10119,1987.*

Tsurutani, B. T., D. J. Southwood, E. J. Smith, and A. Balogh, A survey of low frequency (LF) waves at Jupiter: The Ulysses encounter, *J. Geophys. Res.*, this issue.

S. J. Bame, J. L. Phillips, and M. F. Thomsen, Los Alamos National Laboratory, Los Alamos, NM, 87545.

B. E. Goldstein and E. J. Smith, Jet Propulsion Laboratory, Pasadena, CA9I109.

(Received April 2, 1993;
revised July 6, 1993;
accepted July 9, 1993.)